Long noncoding RNA XIST suppresses tumorigenesis and enhances radiosensitivity in neuroblastoma cells through regulating miR-653-5p/HK2 axis

Liping Mou
People's Hospital of Rizhao

Lili Wang
People's Hospital of Rizhao

Shaoming Zhang
People's Hospital of Rizhao

Qinghua Wang (✉ lwnl5ya@163.com)
People's Hospital of Rizhao   https://orcid.org/0000-0001-6673-1736

Primary research

Abstract

Background

Abnormal expression of long noncoding RNAs (lncRNAs) was often involved in tumorigenesis and radiosensitivity of various cancers. The aim of this study was to explore the biological function and regulatory mechanism of lncRNA X-inactive specific transcript (XIST) in tumorigenesis and radiosensitivity of neuroblastoma.

Methods

The expression of XIST, microRNA-329-3p (miR-653-5p) and hexokinase 2 (HK2) was detected by quantitative real-time polymerase chain reaction (qRT-PCR). Methylthiazolyldiphenyl tetrazolium bromide (MTT) assay, colony formation assay and transwell assay were utilized to detect cell viability, colony formation and cell invasion abilities. Glucose consumption or lactate production was measured by glucose assay kit or lactate assay kit, respectively. The mice xenograft model was established to investigate the role of XIST in vivo. The interaction between miR-653-5p and XIST or HK2 was predicted by starBase v2.0 and verified by dual-luciferase reporter assay. Western blot was used to measure the protein expression of HK2.

Results

XIST and HK2 were highly expressed while miR-653-5p was lowly expressed in neuroblastoma tissues and cells. XIST knockdown inhibited tumorigenesis by repressing cell proliferation and invasion, and increased the radiosensitivity via inhibiting colony formation rates and glycolysis. XIST knockdown also suppressed tumor growth in vivo. Moreover, miR-653-5p could bind to XIST and its downregulation reversed the effects of XIST knockdown on tumorigenesis and radiosensitivity. Additionally, HK2 was a direct target of miR-653-5p and its overexpression attenuated the effects of miR-653-5p restoration on suppression of tumorigenesis and promotion of radiosensitivity. Besides, XIST functioned as a molecular sponge of miR-653-5p to regulate HK2 expression.

Conclusion

XIST interference inhibited tumorigenesis and increased radiosensitivity via regulating miR-653-5p/HK2 axis, providing a novel therapeutic strategy for neuroblastoma.

Background

Neuroblastoma, one of the most frequent extracranial childhood tumors, originates from primitive neural crest cells of the sympathetic nervous system, accounting for 7% of malignant tumors in children and approximately 15% of all childhood cancer deaths [1, 2]. In spite of advances in treatment have improved the survival times of neuroblastoma patients, children with regional or distant metastatic disease still have a poor prognosis [3]. Radiotherapy is the main treatment for tumors, but the efficacy of radiotherapy

in treating neuroblastoma is limited due to obtaining radioresistance in the treatment of this disease [4]. Thus, it is necessary to explain the molecular mechanisms of neuroblastoma and identify more effective therapeutic targets to increase the radiosensitivity.

Long non-coding RNAs (lncRNAs), highly conserved transcripts (> 200 nucleotides), lack protein-coding capacity and play regulatory roles in various physiopathology processes [5]. Currently, numerous studies have demonstrated that lncRNAs are abnormally expressed in a variety of cancers, including neuroblastoma [6]. For instance, lncRNA NBAT-1 downregulation promoted aggressive neuroblastoma through enhancing proliferation and attenuating differentiation of neuronal precursors [7]. Moreover, lncRNA RMRP was overexpressed in neuroblastoma tissues and its knockdown suppressed the progression of neuroblastoma [8]. Importantly, recent researches have proven that lncRNA X-inactive specific transcript (XIST) expression is tightly linked to the progression of multiple cancers, such as lung cancer [9], hepatocellular carcinoma [10] and gastric cancer [11]. Besides, pervious study uncovered that XIST was highly expressed in neuroblastoma tissues and its expression was related to neuroblastoma development [12]. However, the underlying mechanisms of XIST involved in regulating the progression of neuroblastoma and radiosensitivity remain largely unknown.

Increasing evidence revealed that lncRNAs serve as competing endogenous RNAs (ceRNAs) to modulate gene expression through sponging microRNA (miRNA) [13]. MiRNAs are usually small RNAs (18−25 nucleotides) that lack protein-coding potential and negatively gene expression via combining with complementary sequences on target mRNA [14, 15]. Currently, accumulating evidence demonstrated that aberrant expression miRNA was closely related to the development and progression of cancers, and could affect the cells response to radiation [16, 17]. MiR-653-5p has been suggested to function as a tumor suppressor or tumor promoter in different cancers [18, 19]. Moreover, miR-653-5p was also reported to be lowly expressed in neuroblastoma [20]. Nevertheless, the functions of miR-653-5p on the tumorigenesis and radiosensitivity of neuroblastoma are poorly understood.

Several miRNAs target hexokinase 2 (HK2; a metabolism-related factor) to influence the progression of diverse types of cancer [21, 22]. HK2 has been reported to be upregulated in neuroblastoma and acts as a target of miR-143-3p in neuroblastoma [23]. However, there is no report on the interaction between miR-653-5p and HK2, and exact roles of HK2 in neuroblastoma progression and radiosensitivity should be explored.

In the present study, the expression of XIST, miR-653-5p and HK2 was analyzed in neuroblastoma tissues and cells. In addition, we explored their effects on proliferation, invasion, glycolysis, and radiosensitivity, and investigated the regulatory network of XIST/miR-653-5p/HK2 in neuroblastoma cells, aiming to offer a new biological target for treatment of neuroblastoma.

Materials And Methods

Clinical tissue samples

In this study, thirty neuroblastoma tissues and paired normal tissues were obtained from patients undergoing surgery at People's Hospital of Rizhao. The patients did not receive any treatment before surgery. Each patient has signed written informed consent. Excised tissues were collected and promptly frozen in liquid nitrogen, and then cryopreserved at -80°C for subsequent study.

Cell Culture And Transfection

Human embryonic kidney (HEK293) and neuroblastoma cell line (SK-N-BE(2)) were bought from BeNa Culture Collection (Beijing, China). The neuroblastoma cell line (GI-LI-N) was obtained from Conservation Genetics CAS Kunming Cell Bank (Yunnan, China). These cells were cultivated in Dulbecco's modified eagle medium (DMEM; Invitrogen, Waltham, MA, USA) containing 10% fetal bovine serum (FBS; Invitrogen), 100 U/mL penicillin and 100 μg/mL streptomycin. The cells were grown in an incubator of CO_2 (5%) at 37°C.

For this study, small interfering RNA against XIST (si-XIST) and the corresponding control (si-NC), miR-653-5p mimic (miR-653-5p) and the corresponding control (miR-NC), miR-653-5p inhibitor (anti-miR-653-5p) and the corresponding control (anti-miR-NC), XIST or HK2 overexpression plasmid (XIST or HK2) and the corresponding control (pcDNA) were bought from GenePharma (Shanghai, China). Lentivirus-mediated shRNA interference targeting XIST (sh-XIST) and the corresponding control (sh-NC) were constructed by Genechem (Shanghai, China). GI-LI-N and SK-N-BE(2) cells were transfected with oligonucleotide (50 nM) or plasmid (2 μg) using Lipofectamine 3000 (Invitrogen).

Quantitative Real-time Polymerase Chain Reaction (qRT-PCR)

TRIzol reagent (Invitrogen) was applied to isolate total RNA from tissues (neuroblastoma tissues and normal tissues) and cells (HEK293, GI-LI-N and SK-N-BE(2)). Next, the first strand of complementary DNA (cDNA) was synthesized with a High-Capacity cDNA Reverse Transcription Kit and TaqMan MicroRNA Reverse Transcription Kit (Thermo Fisher Scientific, Waltham, MA, USA). The qRT-PCR was carried out using the SYBR Green PCR kit (Thermo Fisher Scientific) on the ABI 7300 system (Thermo Fisher Scientific). In this study, the primers were as follows: XIST (Forward, 5'-CCTCTCCACATACCTCAGT-3'; Reverse, 5'-ACATAATCACACGCATACCA-3'); miR-653-5p (Forward, 5'-CTCAACTGGTGTCGTGGAGTCGGCAATTCAGTTGAGCAGTAGAG-3'; Reverse, 5'-ACACTCCAGCTGGGGTGTTGAAACAATCT-3'); HK2 (Forward, 5'-ACAGCCTGGACGAGAGCATC-3'; Reverse, 5'-AGGTCAAACTCCTCTCGCCG-3'); glyceraldehyde-3-phosphate dehydrogenase (GAPDH) (Forward, 5'-CGCTCTCTGCTCCTCCTGTTC-3'; Reverse, 5'- ATCCGTTGACTCCGACCTTCAC-3'), U6 snRNA (Forward, 5'-CTCGCTTCGGCAGCACATATACT-3'; Reverse, 5'-ACGCTTCACGAATTTGCGTGTC-3'). The XIST, HK2 or miR-653-5p expression was evaluated with the $2^{-\Delta\Delta Ct}$ method, followed by normalizing to GAPDH or U6 snRNA, respectively.

Cell Viability Assay

Methylthiazolyldiphenyl tetrazolium bromide (MTT) was utilized for detecting cell viability. In brief, GI-LI-N and SK-N-BE(2) cells were seeded in 96-well plates and then transfected with si-XIST, si-XIST + anti-miR-

653-5p, miR-653-5p, miR-653-5p + HK2, or matched controls. MTT reagent (5 mg/mL, 10 μL, Beyotime, Shanghai, China) was added to each well after transfection. After incubation for 4 h, the cultured medium from per well would be carefully discarded and dimethyl sulfoxide (150 μL) was added. Lastly, the absorbance was evaluated at 490 nm under a microplate reader (Bio-Rad, Hercules, CA, USA).

Irradiation (IR) And Colony Formation Assay

After transfection for 48 h, GI-LI-N and SK-N-BE(2) cells were placed into six-well plates and the medium was updated every three days. For treatment of IR, cells were exposed to different doses of radiation by a linear accelerator (Varian, Palo Alto, CA, USA) at a dose rate of 3.5 Gy/min. After incubation for 2 weeks, GI-LI-N and SK-N-BE(2) cells were carefully washed with cold phosphate-buffered saline (PBS; pH = 7.2) and subsequently fixed with paraformaldehyde (4%) for 30 min at 4°C. After that, GI-LI-N and SK-N-BE(2) cells were washed by PBS and then stained by crystal violet (0.1%, Sigma-Aldrich, St. Louis, MO, USA). Microscope (Olympus, Tokyo, Japan) was applied to count colonies containing more than 50 cells. The survival fraction was calculated as previously described [24].

Transwell Assay

Transwell assay was performed using a 24-well plate inserts with 8 μm pores (Corning Incorporated, Corning, NY, USA) to evaluate cell invasion capacity. GI-LI-N and SK-N-BE(2) cells (2×10^4 cells/well) re-suspended in DMEM medium alone (100 μL) were placed into the top chamber pre-coated with Matrigel (BD Bioscience, Franklin Lakes, NJ, USA). To induce cells invading through the membrane, the bottom chamber was filled with DMEM containing 10% FBS. After 24 h of incubation, non-invaded cells were carefully removed with cotton bud, and invaded cells were fixed using ethanol (95%) and then stained using crystal violet (0.1%). Finally, a microscope was applied to observe and count invaded cells in five random fields.

Measurement Of Glucose Consumption And Lactate Production

In accordance with the manufacturer's instructions, the glucose consumption and lactate production were detected with the glucose assay kit (Sigma-Aldrich) and lactate assay kit (BioVision, Mountain View, CA, USA), respectively. A standard calibration curve was used for determining the data, followed by normalizing to the amount of total protein.

In vivo tumor growth assay

The sh-XIST or sh-NC was transfected into SK-N-BE(2) cells. Subsequently, stably transfected cells (3×10^6) were subcutaneously injected in BALB/c nude mice (male, 5-week-old, n = 7/group, Huafukang, Beijing, China). From the 8th day, tumor volume was examined using a caliper every 4 days and calculated with the formula: length × width^2/2. From the 10th day, mice were irradiated with 6 Gy X-ray once a week. All mice were sacrificed after injection for 4 weeks, and tumor samples were weighted and collected for detection of XIST level.

Dual-luciferase Reporter Assay

The possible binding sites of miR-653-5p and XIST or HK2 were predicted by starBase v2.0. The XIST and HK2 3'UTR fragments that contained wild-type (WT) or mutant (MUT) binding sites of miR-653-5p were amplified and inserted into pmirGIO luciferase reporter vector (Promega, Madison, WI, USA) to create the WT plasmids (WT-XIST, HK2 3'UTR-WT) or MUT plasmids (MUT-XIST, HK2 3'UTR-MUT). Afterward, GI-LI-N and SK-N-BE(2) cells were co-transfected with reporter plasmids and miR-653-5p or miR-NC. After incubating the cells for 48 h, the luciferase activity was estimated via Dual-Luciferase Reporter assay system (Promega).

Western Blot Assay

Transfected cells were lysed using RIPA lysis buffer (Sigma-Aldrich) supplemented with 1 mM phenylmethylsulphonyi fluoride (PMSF; Sigma-Aldrich) to extract the total protein. After quantification by using bicinchoninic acid protein assay kit (Tanon, Shanghai, China), 30 μg of protein in each group was separated using sodium dodecyl sulfate-polyacrylamide gel electrophoresis (SDS-PAGE). After that, polyvinylidene fluoride (Beyotime) membranes were employed to transfer the protein. After blocking with 5% non-fat milk in PBS containing 0.05% Tween 20 (PBST), the membranes were immunoblotted by primary antibody against HK2 (1:5000, ab227198, Abcam, Cambridge, UK) or GAPDH (1:2500, ab9485, Abcam) for 12–16 h at 4°C. Afterward, membranes were maintained in horseradish peroxidase-conjugated anti-rabbit IgG (1:4000, D110058, Sangon Biotech, Shanghai, China) after washing with PBST. Immunoreactive bands were visualized through the enhanced chemiluminescence (ECL; Tanon) reagent following the manufacturer's protocol. ImageJ software was utilized to quantify the protein expression. GAPDH was used as an internal control.

Statistical analysis

All data in this study were displayed as mean ± standard deviation (SD) and all experiments were repeated at least 3 times. Correlation between miR-653-5p and XIST or HK2 was detected by Spearman rank correlation. The results from different groups were assessed using the two-tailed Student's t-test (for two groups) and a one-way analysis of variance (ANOVA; for more than two groups). Statistical analyses were performed using Graphpad Prism version 6.0 software (GraphPad Software, San Diego California, USA). $P < 0.05$ indicates a statistically significant result.

Results

XIST was upregulated and miR-653-5p was downregulated in neuroblastoma tissues and cells

Firstly, we explored the expression of XIST and miR-653-5p in neuroblastoma tissues and cells by qRT-PCR. As presented in Fig. 1A and 1B, XIST was overexpressed in neuroblastoma tissues and cells in contrast to their matched controls. Moreover, we found that the abundance of miR-653-5p was decreased in neuroblastoma tissues and cells with respect to their corresponding controls (Fig. 1C and 1D). Besides,

the correlation between of XIST and miR-653-5p was analyzed in neuroblastoma tissues. As depicted in Fig. 1E, XIST expression was negatively correlated with miR-653-5p in neuroblastoma tissues (r=-0.8114, p < 0.001). These data indicated that XIST and miR-653-5p might be involved in the pathogenesis of neuroblastoma.

XIST knockdown inhibited cell proliferation and invasion, and enhanced radiosensitivity by inhibiting glycolysis in neuroblastoma cells

Next, the effects of XIST on cell proliferation, invasion, glycolysis, and radiosensitivity were investigated using loss-function experiments. The transfection efficiency of si-XIST was determined by qRT-PCR. The results showed that the expression of XIST was decreased in GI-LI-N and SK-N-BE(2) cells transfected with si-XIST relative to those cells transfected with si-NC or control cells (Fig. 2A), suggesting the transfection of si-XIST was successful. MTT analysis revealed that XIST interference inhibited the viability of GI-LI-N and SK-N-BE(2) cells (Fig. 2B and 2C). Moreover, colony formation assay indicated that XIST deficiency decreased the number of colonies in GI-LI-N and SK-N-BE(2) cells (Fig. 2D). Furthermore, silencing XIST repressed the invasion ability of GI-LI-N and SK-N-BE(2) cells (Fig. 2E). GI-LI-N and SK-N-BE(2) cells were transfected with si-XIST or si-NC and then irradiated with 0 Gy to 8 Gy to explore the effect of XIST on radiosensitivity. The data showed that XIST downregulation strikingly decreased the survival fraction of GI-LI-N and SK-N-BE(2) cells exposed to radiation compared to si-NC or control group (Fig. 2F and 2G). Most cancer cells mainly rely on aerobic glycolysis to produce the energy needed for cellular processes [25]. This aerobic glycolysis will result in increased glucose consumption and lactate production. We observed that knockdown of XIST inhibited glucose consumption and lactate production in GI-LI-N and SK-N-BE(2) cells (Fig. 2H and 2I). Moreover, we found that glucose consumption and lactate production were decreased in GI-LI-N and SK-N-BE(2) cells treated with 2-deoxyglucose (2-DG; glycolytic inhibitor) (Fig. 2J and 2K). QRT-PCR analysis showed that the expression of XIST was enhanced in cells transfected with XIST compared to pcDNA group (Fig. 2L). Besides, the promotive effect of XIST on cell survival fraction was overturned by treatment with 2-DG (Fig. 2M and 2N), suggesting that XIST knockdown enhanced the radiosensitivity through inhibition of glycolysis. Taken together, these results demonstrated that XIST interference inhibited the tumorigenesis and increased the radiosensitivity in neuroblastoma cells.

Downregulation of XIST inhibited tumor growth through increasing radiosensitivity in vivo

To explore the impact of XIST on tumor growth and radiation response in vivo, we established a xenograft model in which the SK-N-BE(2) cells stably transfected with sh-XIST or sh-NC were subcutaneously injected into BALB/c nude mice and irradiated with 6 Gy X-ray once a week. In line with in vitro results, combination of XIST interference and IR treatment significantly inhibited tumor volume and weight in xenograft model compared with only IR group (Fig. 3A and 3B). In addition, knockdown of XIST and IR treatment obviously decreased the expression of XIST in excised tumor masses relative to only IR group (Fig. 3C). These above findings indicated that downregulation of XIST could enhance the radiosensitivity to inhibit tumor growth in vivo.

XIST Directly Interacted With Mir-653-5p In Neuroblastoma Cells

In view of the alteration of XIST and miR-653-5p in neuroblastoma tissues and cell lines, as well as the negative correction between XIST and miR-653-5p expression, we wondered whether the function of XIST was mediated by miR-653-5p through complementary binding sites. StarBase v2.0 predicted that XIST contained putative binding sites of miR-653-5p (Fig. 4A). To verify whether miR-653-5p was a direct target of XIST, the dual-luciferase reporter assay was performed. As presented in Fig. 4B and 4C, overexpression of miR-653-5p led to a significant decrease in the luciferase activity of WT-XIST, while luciferase activity of MUT-XIST was not evidently affected after transfection with miR-653-5p in GI-LI-N and SK-N-BE(2) cells. And we found that the expression of XIST was reduced in GI-LI-N and SK-N-BE(2) cells transfected with si-XIST, while its expression was elevated in cells transfected with XIST (Fig. 4D). Next, we explored the effect of XIST on expression of miR-653-5p. As expected, knockdown of XIST increased the expression of miR-653-5p, whereas overexpression of XIST presented an opposite effect (Fig. 4E). At the same time, we observed that co-transfection of anti-miR-653-5p and si-XIST abated the effect of si-XIST on promotion of miR-653-5p expression (Fig. 4F). Additionally, deficiency of miR-653-5p reversed the inhibitory effects of XIST knockdown on viability, colony formation and invasion of GI-LI-N and SK-N-BE(2) cells (Fig. 4G-4J). Moreover, the suppressive effect of XIST interference on the survival fraction was weakened by downregulation of miR-653-5p in GI-LI-N and SK-N-BE(2) cells exposed to IR (Fig. 4K and 4L). Furthermore, inhibition of miR-653-5p attenuated the repressive impact of XIST knockdown on glucose consumption and lactate production (Fig. 4M and 4N). Our findings suggested that miR-653-5p could bind to XIST and its knockdown reversed the effects of XIST interference on tumorigenesis and radiosensitivity in neuroblastoma cells.

HK2 was a direct target of miR-653-5p in neuroblastoma cells

To explore the underlying mechanism of miR-653-5p in progression of neuroblastoma, the function targets of miR-653-5p were searched by starBase v2.0. As presented in Fig. 5A, HK2 was predicted to be a target of miR-653-5p. Then dual-luciferase reporter assay displayed that the luciferase activity of HK2 3'UTR-WT could be obviously inhibited by transfection of miR-653-5p, whereas no clear change of the luciferase activity of HK2 3'UTR-MUT was found (Fig. 5B and 5C). Next, we detected the expression of HK2 in neuroblastoma tissues and cells. The results suggested that the mRNA and protein expression of HK2 were increased in neuroblastoma tissues in comparison with normal tissues (Fig. 5D and 5E). Additionally, HK2 expression was negatively correlated with miR-653-5p level in neuroblastoma tissues (r=-0.5985, p < 0.001) (Fig. 5F). Likewise, the mRNA and protein abundance of HK2 were also enhanced in neuroblastoma cells (GI-LI-N and SK-N-BE(2)) compared to HEK293 cells (Fig. 5G and 5H). These data illustrated that miR-653-5p directly interacted with HK2.

Overexpression of HK2 reversed the effects of miR-653-5p on inhibition of tumorigenesis and promotion of radiosensitivity in neuroblastoma cells

To determine whether the effects of miR-653-5p were regulated by HK2 expression, GI-LI-N and SK-N-BE(2) cells were transfected with miR-NC, miR-653-5p, miR-653-5p + pcDNA, or miR-653-5p + HK2.

Western blot showed that HK2 protein expression was decreased in cells transfected with miR-653-5p, while the effect was abated by co-transfection of HK2 (Fig. 6A). Additionally, overexpression of miR-653-5p reduced the cell viability, colony formation and invasion of GI-LI-N and SK-N-BE(2) cells, which was reversed by upregulating HK2 (Fig. 6B-6E). Moreover, the effects of miR-653-5p restoration on inhibition of survival fraction and glycolysis were also overturned by overexpression of HK2 (Fig. 6F-6I). Collectively, these findings demonstrated that miR-653-5p exerted its biological functions through regulating HK2 expression.

HK2 was regulated by XIST and miR-653-5p in neuroblastoma cells

To explore whether XIST served as a ceRNA of miR-653-5p to modulate HK2 expression, GI-LI-N and SK-N-BE(2) cells were transfected with si-NC, si-XIST, si-XIST + anti-miR-NC, or si-XIST + anti-miR-653-5p. Western blot assay demonstrated that the protein level of HK2 was decreased after transfection of si-XIST, while the effect was reversed by co-transfection of anti-miR-653-5p (Fig. 7A and 7B). In a word, our results proved that XIST regulated HK2 expression by sponging miR-653-5p in neuroblastoma cells.

Discussion

Neuroblastoma is considered to be a common and aggressive malignancy in children. Recently, it has been increasingly recognized that dysregulation of lncRNAs is involved in the progression of neuroblastoma [23, 26]. Radiotherapy has become an effective strategy for neuroblastoma treatment, however, the influence of lncRNAs on radiosensitivity of neuroblastoma cells is not well elucidated. The purpose of this research was to explore the effects of XIST on neuroblastoma progression and radiosensitivity.

Up to now, a growing number of researches have shown that XIST serves as an oncogene and plays essential roles in cellular behaviors, such as cell growth, cell cycle, metastasis and apoptosis [27, 28]. Besides, Song et al. pointed out that XIST was overexpressed in nasopharyngeal carcinoma tissues, and accelerated nasopharyngeal carcinoma cell growth through targeting miR-34a-5p [29]. Moreover, Chen et al. uncovered that XIST knockdown inhibited colorectal cancer cell proliferation and metastasis via sponging miR-200b-3p to decrease ZEB1 expression [30]. In our research, it was found that XIST abundance was elevated in neuroblastoma tissues and cells. Additionally, interference of XIST suppressed cell proliferation and invasion, and elevated radiosensitivity via suppressing glycolysis in neuroblastoma cells as well as restrained tumor growth through enhancing radiosensitivity in vivo. In agreement with our findings, Zhang et al. disclosed that XIST expression was markedly enhanced in neuroblastoma tissues and its knockdown inhibited the cell growth and metastasis in neuroblastoma cells by regulating H3 histone methylation of DKK1 [12]. These results revealed that XIST was involved in the tumorigenesis of neuroblastoma and could enhance radiosensitivity.

Precious research has shown that miR-653-5p has pivotal roles in the regulating cellular behaviors, such as proliferation, cell cycle and apoptosis [31]. It has recently been identified as a cancer-related miRNA for several cancers. For example, Fu et al. declared that miR-653-5p was highly expressed in prostate cancer

tissues, and miR-653-5p inhibition limited prostate cancer cell proliferation and metastasis via inhibiting Wnt/β-catenin signaling [32]. Han, et al. proved that miR-653-5p acted as a tumor-suppressive miRNA through targeting TIAM1 to suppress lung cancer cell proliferation and invasion [33]. These findings suggested that miR-653-5p could exert a tumor-suppressive or tumor-promotive function depending on the type of cancer. More importantly, Chi et al. showed that miR-653-5p expression was reduced in neuroblastoma tissues, and miR-653-5p knockdown reversed the inhibitory abilities of cell proliferation, migration, and invasion induced by downregulating SNHG7 in neuroblastoma cells, suggesting that miR-653-5p might act as a tumor suppressor in neuroblastoma [20]. Here, we found that miR-653-5p abundance was declined in neuroblastoma tissues and cells, and was inversely correlated with XIST. Previous studies have demonstrated that lncRNAs can execute their functions through binding with their downstream miRNAs [34]. To further explore the relationship between XIST and miR-653-5p, starBase v2.0 was used to predict the targeting relationship. Interestingly, starBase v2.0 showed that miR-653-5p contained predicted binding sites with XIST. Next, the prediction was validated through dual-luciferase reporter assay. In addition, rescue experiments demonstrated that miR-653-5p knockdown could reverse the impact of XIST interference on cell proliferation, invasion, radiosensitivity, and glycolysis in neuroblastoma cells. Collectively, our data indicated that XIST exerted its function through regulating miR-653-5p expression.

It is well known that the biological functions of miRNAs are realized via modulating mRNA expression, so the potential target genes for miR-653-5p would be analyzed in further analysis. Despite the fact that numerous tumor-associated genes were predicted using starBase v2.0, HK2 was selected as the candidate target gene of miR-653-5p due to its tumor-promoting effect. Further, dual-luciferase reporter assay proved that miR-653-5p directly targeted HK2. HK2 (a major type of hexokinase family) was reported to be overexpressed and facilitated rates of glucose metabolism necessary for tumor growth in multiple cancers [35, 36]. In addition, Botzer et al. presented that high expression of HK2 promoted neuroblastoma metastasis [37]. Besides, Cen et al. revealed that HK2 was upregulated in neuroblastoma tissues and cells, and HK2 accumulation weakened the repressive effects of miR-143-3p restoration on progression of neuroblastoma [23]. In line with previous findings, we also demonstrated that HK2 was highly expressed in neuroblastoma tissues and cells. Moreover, HK2 upregulation could weaken the influence of miR-653-5p restoration on inhibition of tumorigenesis and promotion of radiosensitivity in neuroblastoma cells. Furthermore, we uncovered that XIST acted as a molecular sponge of miR-653-5p to modulate HK2 expression. In a word, these findings disclosed that XIST regulated the progression and radiosensitivity of neuroblastoma cells by sponging miR-653-5p to modulate HK2 expression.

Conclusion

XIST and HK2 were upregulated while miR-653-5p was downregulated in neuroblastoma tissues and cells. Knockdown of XIST inhibited the tumorigenesis and enhanced the radiosensitivity in neuroblastoma cells by regulating miR-653-5p and HK2 expression. These findings might provide a potential therapeutic strategy for neuroblastoma.

Abbreviations

lncRNAs: long noncoding RNAs; XIST: X-inactive specific transcript; miR-653-5p: microRNA-329-3p; HK2: hexokinase 2; qRT-PCR: quantitative real-time polymerase chain reaction; MTT: Methylthiazolyldiphenyl tetrazolium bromide; ceRNAs: competing endogenous RNAs; miRNA: microRNA; PBS: phosphate-buffered saline; WT: wild-type; MUT: mutant

Declarations

Ethics approval and consent to participate

All the cervical cancer tissues samples were collected with written informed consent in accordance with the Declaration of Helsinki and with the approval of the Ethics Committee of People's Hospital of Rizhao (No. SU493565, Date: 2019/01/22, Shandong, China).

Animal studies were performed in compliance with the ARRIVE guidelines and the Basel Declaration.Experimental procedures were approved by the Institutional and Local Committee on the Care and Use of Animals of People's Hospital of Rizhao (ACU146379) on January 25, 2019. All animals received humane care according to the National Institutes of Health (USA) guidelines.

Consent for publication

Not applicable

Availability of data and materials

The data sets used and/or analyzed during the current study are available from the corresponding author on reasonable request.

Competing interests

The authors declare that they have no competing interests.

Funding

None.

Authors' contributions

Liping Mou participated in the conception and design of the study. Lili Wang performed the analysis and interpretation of data. Shaoming Zhang contributed to drafting the manuscript. Qinghua Wang reviewed and approved the final submitted manuscript.

Acknowledgment

References

1. Matthay KK. Neuroblastoma: biology and therapy. 1997, 11(12):1857.

2. Ward E, DeSantis C, Robbins A, Kohler B, Jemal A. Childhood and adolescent cancer statistics, 2014. CA Cancer J Clin. 2014, 64(2):83-103.

3. Harrison J, Myers M, Rowen M, Vermund H. Results of combination chemotherapy, surgery, and radiotherapy in children with neuroblastoma. Cancer. 1974, 34(3):485-90.

4. Madhusoodhanan R, Natarajan M, Veeraraghavan J, Herman TS, Jamgade A, Singh N, Aravindan N. NFκB signaling related molecular alterations in human neuroblastoma cells after fractionated irradiation. J Radiat Res (Tokyo). 2009, 50(4):311-24.

5. Wilusz JE, Hongjae S, Spector DL. Long noncoding RNAs: functional surprises from the RNA world. Genes Dev. 2009, 23(13):1494-504.

6. Prensner JR, Chinnaiyan AM. The emergence of lncRNAs in cancer biology. Cancer Discov. 2011, 1(5):391-407.

7. Pandey GK, Mitra S, Subhash S, Hertwig F, Kanduri M, Mishra K, Fransson S, Ganeshram A, Mondal T, Bandaru S. The risk-associated long noncoding RNA NBAT-1 controls neuroblastoma progression by regulating cell proliferation and neuronal differentiation. Cancer Cell. 2014, 26(5):722-37.

8. Pan J, Zhang D, Zhang J, Qin P, Wang J. LncRNA RMRP silence curbs neonatal neuroblastoma progression by regulating microRNA-206/tachykinin-1 receptor axis via inactivating extracellular signal-regulated kinases. Cancer Biol Ther. 2019, 20(5):653-65.

9. Fang J, Sun C-C, Gong C. Long noncoding RNA XIST acts as an oncogene in non-small cell lung cancer by epigenetically repressing KLF2 expression. Biochem Biophys Res Commun. 2016, 478(2):811-7.

10. Zhuang LK, Yang YT, Ma X, Han B, Wang ZS, Zhao QY, Wu LQ, Qu ZQ. MicroRNA-92b promotes hepatocellular carcinoma progression by targeting Smad7 and is mediated by long non-coding RNA XIST. Cell Death Dis. 2016, 7:e2203.

11. Chen D-l, Ju H-q, Lu Y-x, Chen L-z, Zeng Z-l, Zhang D-s, Luo H-y, Wang F, Qiu M-z, Wang D-s. Long non-coding RNA XIST regulates gastric cancer progression by acting as a molecular sponge of miR-101 to modulate EZH2 expression. J Exp Clin Cancer Res. 2016, 35(1):142.

12. Zhang J, Li W-y, Yang Y, Yan L-z, Zhang S-y, He J, Wang J-x. LncRNA XIST facilitates cell growth, migration and invasion via modulating H3 histone methylation of DKK1 in neuroblastoma. Cell Cycle. 2019(just-accepted).

13. Bach DH, Lee SK, Sood AK. Circular RNAs in Cancer. Mol Ther Nucleic Acids. 2019, 16:118-29.

14. Ardekani AM, Naeini MM. The role of microRNAs in human diseases. Avicenna J Med Biotechnol. 2010, 2(4):161-79.

15. Jansson MD, Lund AH. MicroRNA and cancer. Mol Oncol. 2012, 6(6):590-610.

16. Dickey JS, Zemp FJ, Martin OA, Kovalchuk O. The role of miRNA in the direct and indirect effects of ionizing radiation. Radiat Environ Biophys. 2011, 50(4):491.

17. Reddy KB. MicroRNA (miRNA) in cancer. Cancer Cell Int. 2015, 15(1):38.

18. Su Y, Feng W, Zhong G, Ya Y, Du Z, Shi J, Chen L, Dong W, Lin T. ciRs-6 upregulates March1 to suppress bladder cancer growth by sponging miR-653. Aging (Albany NY). 2019, 11(23):11202-23.

19. Xie R, Tang J, Zhu X, Jiang H. Silencing of hsa_circ_0004771 inhibits proliferation and induces apoptosis in breast cancer through activation of miR-653 by targeting ZEB2 signaling pathway. Biosci Rep. 2019, 39(5):BSR20181919.

20. Chi R, Chen X, Liu M, Zhang H, Li F, Fan X, Wang W, Lu H. Role of SNHG7-miR-653-5p-STAT2 feedback loop in regulating neuroblastoma progression. J Cell Physiol. 2019, 234(8):13403-12.

21. Yoshino H, Enokida H, Itesako T, Kojima S, Kinoshita T, Tatarano S, Chiyomaru T, Nakagawa M, Seki N. Tumor-suppressive micro RNA-143/145 cluster targets hexokinase-2 in renal cell carcinoma. Cancer Sci. 2013, 104(12):1567-74.

22. Fang R, Xiao T, Fang Z, Sun Y, Li F, Gao Y, Feng Y, Li L, Wang Y, Liu X. MicroRNA-143 (miR-143) regulates cancer glycolysis via targeting hexokinase 2 gene. J Biol Chem. 2012, 287(27):23227-35.

23. Cen Y, Xu L, Huang S, Zhuang S. miR-143-3p functions as a tumor suppressor by targeting HK2 in neuroblastomas. Int J Clin Exp Med. 2019, 12(7):8450-60.

24. Zhou S, Ye W, Ren J, Shao Q, Qi Y, Liang J, Zhang M. MicroRNA-381 increases radiosensitivity in esophageal squamous cell carcinoma. Am J Cancer Res. 2015, 5(1):267.

25. Hsu PP, Sabatini DM. Cancer cell metabolism: Warburg and beyond. Cell. 2008, 134(5):703-7.

26. Bevilacqua V, Gioia U, Di Carlo V, Tortorelli AF, Colombo T, Bozzoni I, Laneve P, Caffarelli E. Identification of linc-NeD125, a novel long non coding RNA that hosts miR-125b-1 and negatively controls proliferation of human neuroblastoma cells. RNA Biol. 2015, 12(12):1323-37.

27. Jiang H, Zhang H, Hu X, Li W. Knockdown of long non-coding RNA XIST inhibits cell viability and invasion by regulating miR-137/PXN axis in non-small cell lung cancer. Int J Biol Macromol. 2018, 111:623-31.

28. Song H, He P, Shao T, Li Y, Li J, Zhang Y. Long non-coding RNA XIST functions as an oncogene in human colorectal cancer by targeting miR-132-3p. J BUON. 2017, 22(3):696-703.

29. Song P, Ye LF, Zhang C, Peng T, Zhou XH. Long non-coding RNA XIST exerts oncogenic functions in human nasopharyngeal carcinoma by targeting miR-34a-5p. Gene. 2016, 592(1):8-14.

30. Chen D-l, Chen L-z, Lu Y-x, Zhang D-s, Zeng Z-l, Pan Z-z, Huang P, Wang F-h, Li Y-h, Ju H-q. Long noncoding RNA XIST expedites metastasis and modulates epithelial−mesenchymal transition in colorectal cancer. Cell Death Dis. 2017, 8(8):e3011.

31. Cao Y-L, Dong W, Li Y-Z, Han W. MicroRNA-653 Inhibits Thymocyte Proliferation and Induces Thymocyte Apoptosis in Mice with Autoimmune Myasthenia Gravis by Downregulating TRIM9. Neuroimmunomodulation. 2019, 26(1):7-18.

32. Fu Q, Sun Z, Yang F, Mao T, Gao Y, Wang H. SOX30, a target gene of miR-653-5p, represses the proliferation and invasion of prostate cancer cells through inhibition of Wnt/β-catenin signaling. Cell Mol Biol Lett. 2019, 24(1):1-13.

33. Han W, Wang L, Zhang L, Wang Y, Li Y. Circular RNA circ-RAD23B promotes cell growth and invasion by miR-593−3p/CCND2 and miR-653−5p/TIAM1 pathways in non-small cell lung cancer. Biochem Biophys Res Commun. 2019, 510(3):462-6.

34. Jin B, Jin H, Wu HB, Xu JJ, Li B. Long non-coding RNA SNHG15 promotes CDK14 expression via miR-486 to accelerate non-small cell lung cancer cells progression and metastasis. J Cell Physiol. 2018, 233(9):7164-72.

35. He H-c, Bi X-c, Zheng Z-w, Dai Q-s, Han Z-D, Liang Y-X, Ye Y-K, Zeng G-h, Zhu G. Real-time quantitative RT-PCR assessment of PIM-1 and hK2 mRNA expression in benign prostate hyperplasia and prostate cancer. Med Oncol. 2009, 26(3):303-8.

36. Mathupala S, Ko Ya, Pedersen PL. Hexokinase II: cancer's double-edged sword acting as both facilitator and gatekeeper of malignancy when bound to mitochondria. Oncogene. 2006, 25(34):4777.

37. Botzer LE, Maman S, Sagi-Assif O, Meshel T, Nevo I, Yron I, Witz IP. Hexokinase 2 is a determinant of neuroblastoma metastasis. Br J Cancer. 2016, 114(7):759.
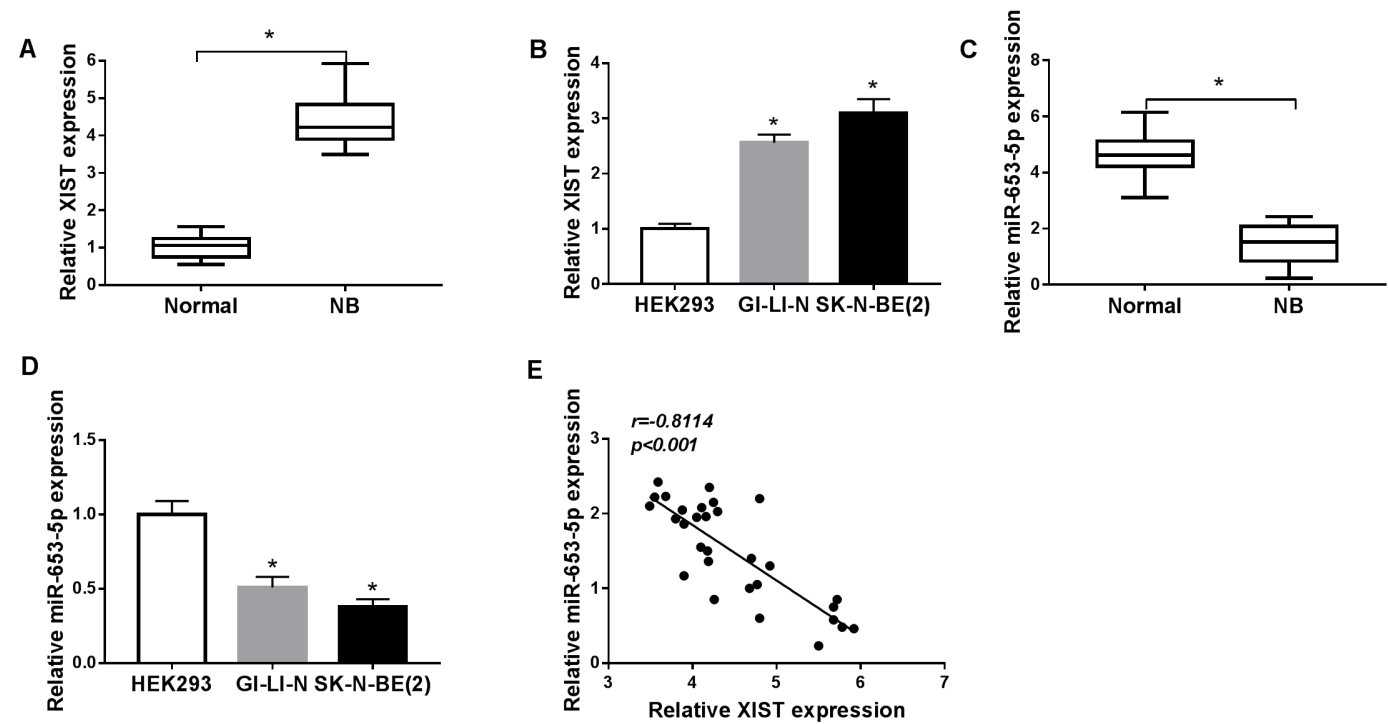
Figures

Figure 1

XIST was upregulated while miR-653-5p was downregulated in neuroblastoma tissues and cell lines. (A and B) Relative XIST expression was detected by qRT-PCR in neuroblastoma tissues, normal tissues, neuroblastoma cells (GI-LI-N and SK-N-BE(2)) and HEK293 cells. (C and D) Relative miR-653-5p expression was measured by qRT-PCR in neuroblastoma tissues, normal tissues, neuroblastoma cells (GI-LI-N and SK-N-BE(2)) and HEK293 cells. (E) Correlation between XIST and miR-653-5p expression was verified by Spearman rank correlation. *P<0.05.
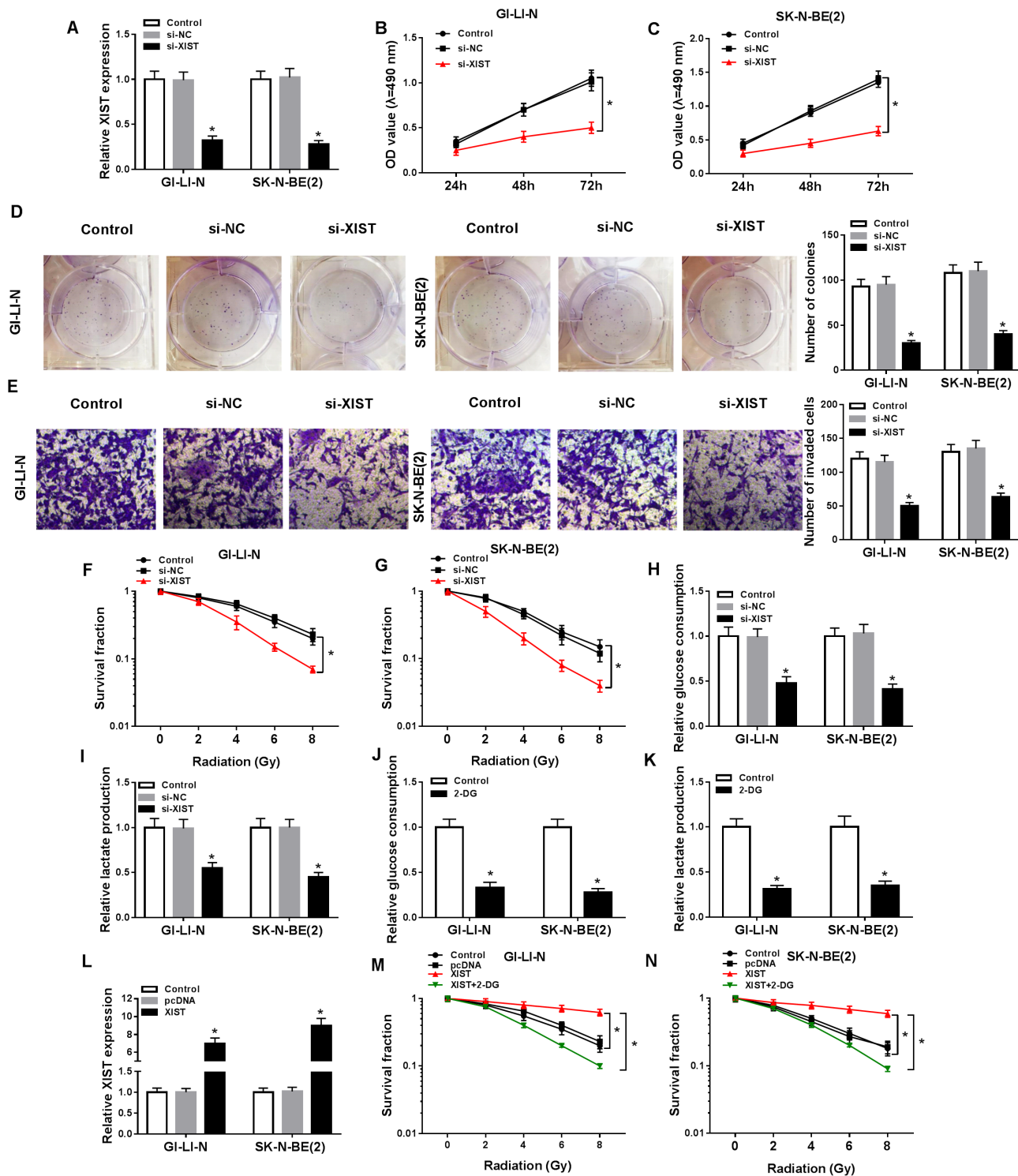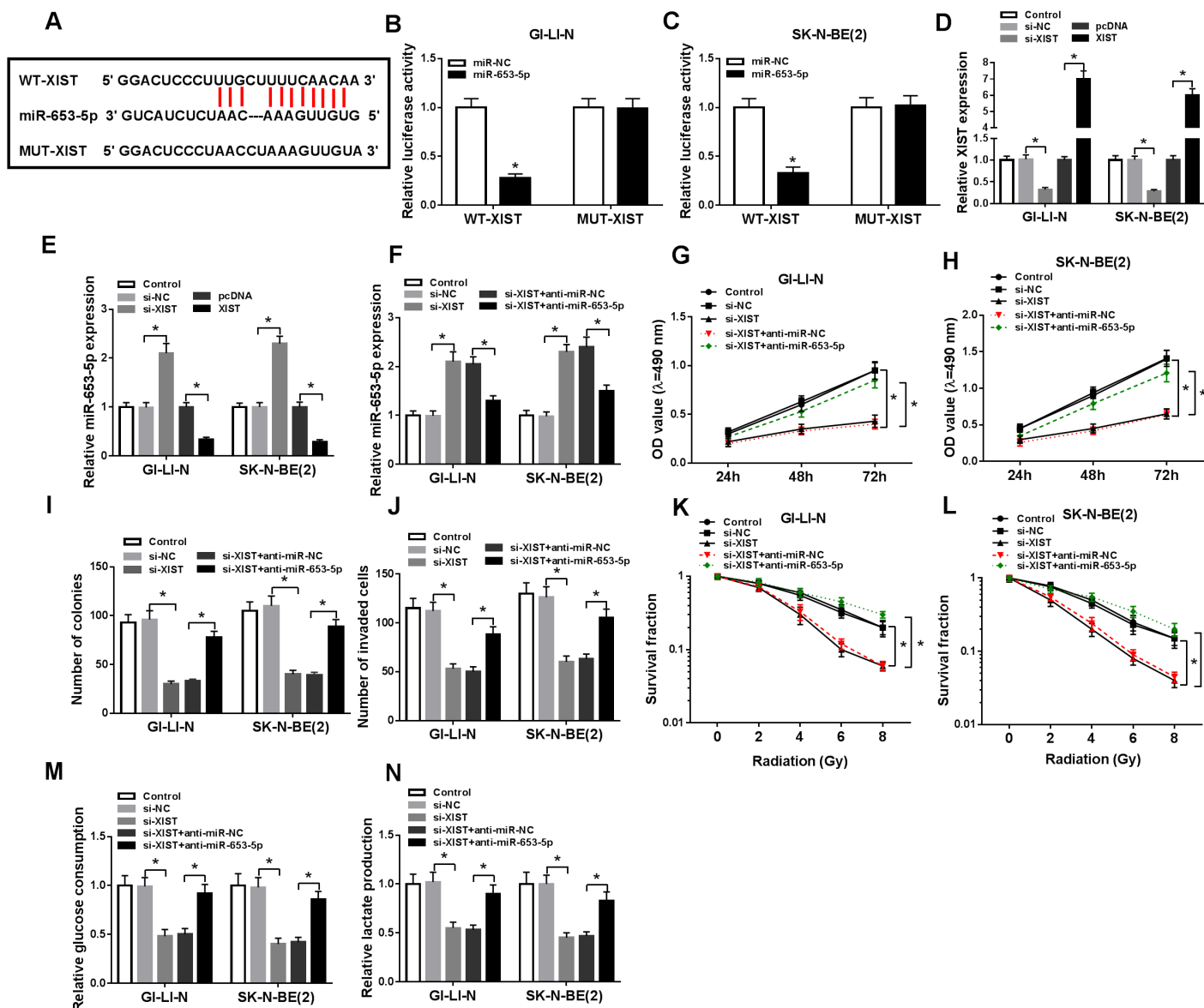

Figure 2

XIST knockdown suppressed cell proliferation and invasion, and promoted radiosensitivity through inhibiting glycolysis in neuroblastoma cells. (A-E) GI-LI-N and SK-N-BE(2) cells were divided into 3 groups: Control, si-NC, and si-XIST. (A) The expression of XIST was examined using qRT-PCR analysis. (B and C) MTT assay was employed to analyze cell viability. (D) Colony formation assay was utilized to determine the number of colonies. (E) Cell invasion was detected by transwell assay. (F and G) Cell survival fraction was detected by colony formation assay in GI-LI-N and SK-N-BE(2) cells transfected with si-NC or si-XIST and exposed to radiation. (H-K) Glucose consumption and lactate production were measured in GI-LI-N and SK-N-BE(2) cells transfected with si-NC or si-XIST as well as the cells treated with 2-DG by glucose assay kit and lactate assay kit, respectively. (L) The expression of XIST was analyzed in GI-LI-N and SK-N-BE(2) cells transfected with pcDNA or XIST using qRT-PCR analysis. (M and N) Colony formation assay was applied to determine cell survival fraction in LI-N and SK-N-BE(2) cells transfected with si-NC or si-XIST or si-XIST + 2-DG under radiation condition. *P<0.05.
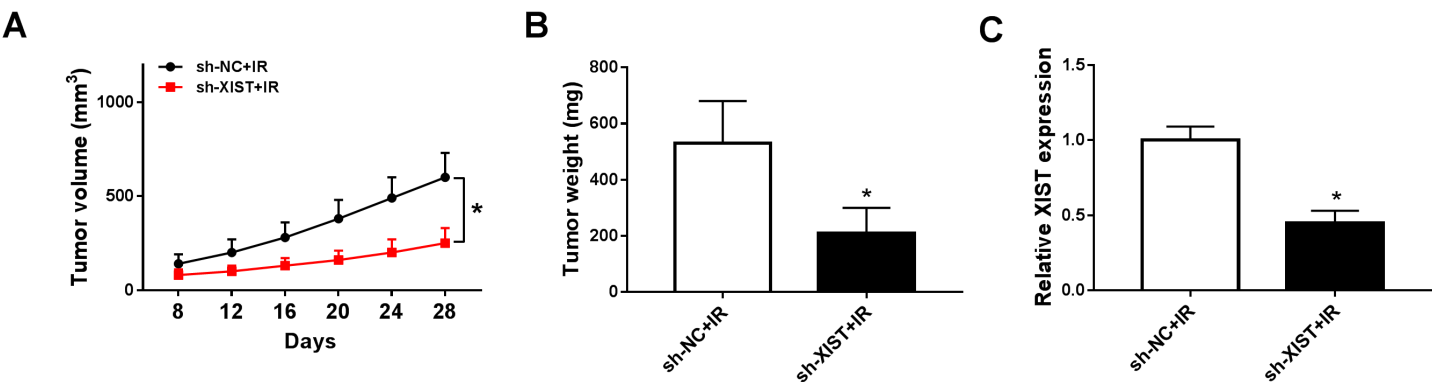
Figure 3

Interference of XIST inhibited tumor growth via enhancing radiosensitivity in vivo. SK-N-BE(2) cells transfected with sh-NC or sh- XIST were injected subcutaneously into nude mice, and the mice were treated with IR. (A and B) Tumor volume and weight were detected. (C) Relative expression of XIST was analyzed by qRT-PCR in resected tumor tissues. *P<0.05.

Figure 4

XIST knockdown inhibited tumorigenesis and promoted radiosensitivity in neuroblastoma cells by sponging miR-653-5p. (A) Predicted binding sites between miR-653-5p and XIST were shown. (B and C) Dual-luciferase reporter assay was conducted to determine luciferase activity in GI-LI-N and SK-N-BE(2) cells co-transfected with miR-653-5p or miR-NC and WT-XIST or MUT-XIST. (D and E) XIST and miR-653-5p expression were detected through qRT-PCR analysis in GI-LI-N and SK-N-BE(2) cells transfected with si-NC, si-XIST, pcDNA, or XIST. (F-N) GI-LI-N and SK-N-BE(2) cells were transfected with si-NC, si-XIST, si-XIST + anti-miR-NC, or si-XIST + anti-miR-653-5p. (F) The abundance of miR-653-5p was measured by qRT-PCR. (G and H) MTT assay was performed to examine cell viability. (I) The number of colonies was determined by colony formation assay. (J) Transwell assay was carried out to detect the number of invaded cells. (K and L) Cell survival fraction was determined by colony formation assay under radiation

condition. (M and N) Glucose consumption or lactate production was measured by glucose assay kit or lactate assay kit, respectively. *P<0.05.
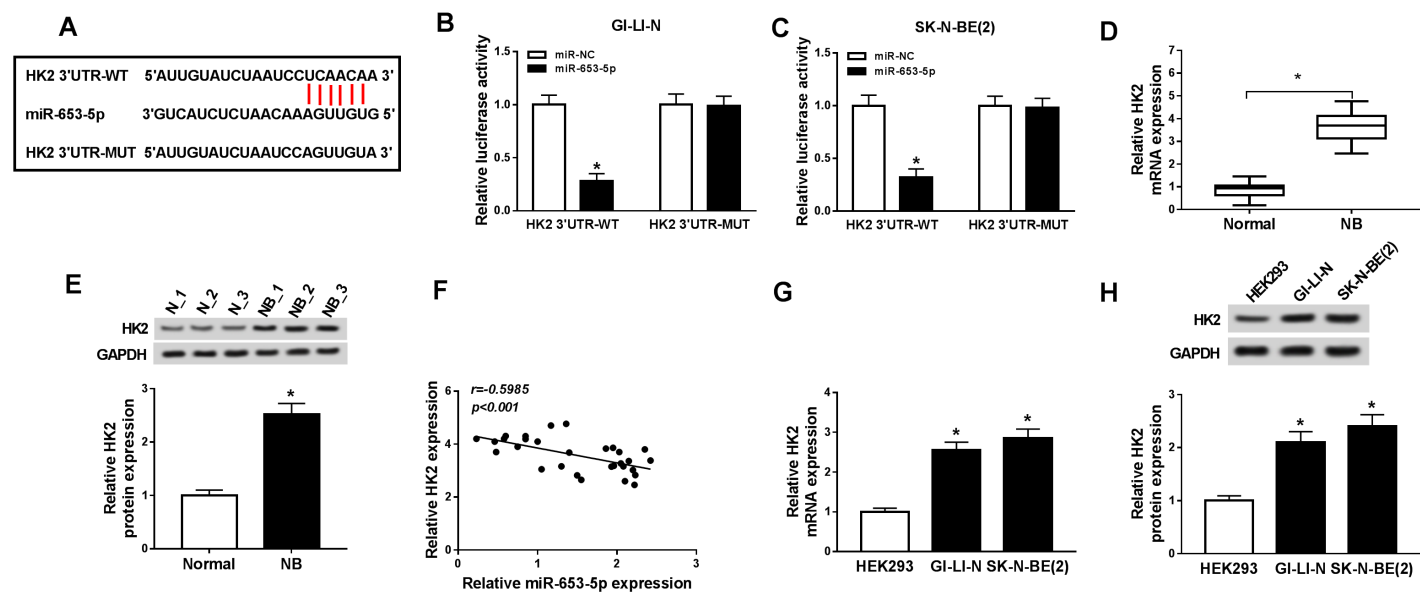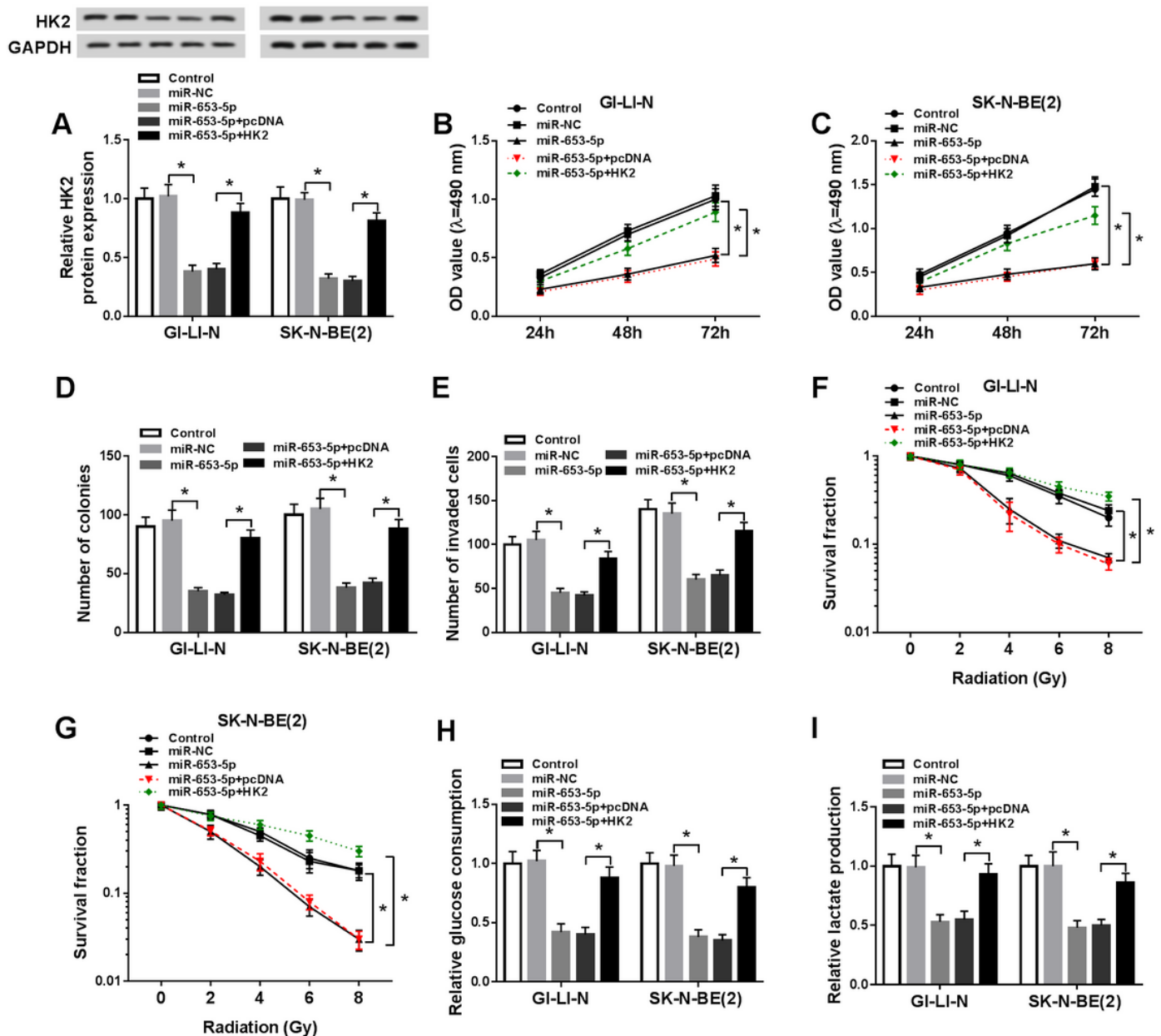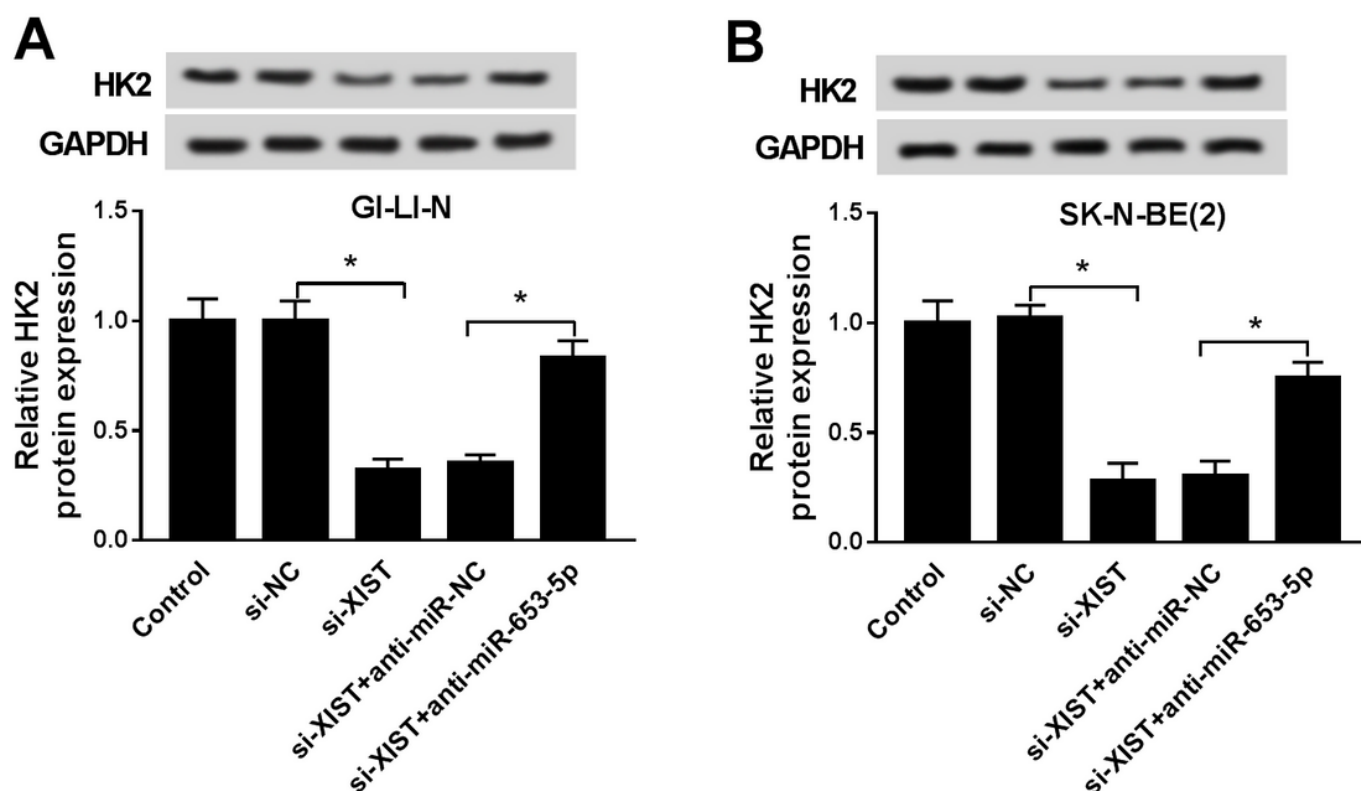

Figure 5

HK2 was a downstream target of miR-653-5p in neuroblastoma cells. (A) The putative binding sites between miR-653-5p and HK2 were predicted by starBase v2.0. (B and C) Relative luciferase activity was determined in GI-LI-N and SK-N-BE(2) cells co-transfected with HK2 3'UTR-WT or HK2 3'UTR-MUT and miR-653-5p or miR-NC. (D and E) The mRNA and protein expression of HK2 were evaluated in neuroblastoma tissues and normal tissues by qRT-PCR and western blot analysis, respectively. (F) Correlation between HK2 and miR-653-5p expression was determined by Spearman rank correlation. (G and H) The mRNA and protein expression of HK2 were assessed in neuroblastoma cells (GI-LI-N and SK-N-BE(2)) and HEK293 cells by qRT-PCR and western blot, respectively. *P<0.05.

Figure 6

Overexpression of miR-653-5p suppressed tumorigenesis and increased radiosensitivity in neuroblastoma cells by downregulating HK2. GI-LI-N and SK-N-BE(2) cells were divided into 5 groups: Control, miR-NC, miR-653-5p, miR-653-5p + pcDNA, and miR-653-5p + HK2. (A) The protein abundance of HK2 was detected by western blot assay. (B and C) Cell viability was evaluated by MTT assay. (D) The number of colonies was determined using colony formation assay. (E) Transwell assay was performed to assess cell invasion ability. (F and G) Cell survival fraction was measured by colony formation assay under radiation condition. (H and I) Glucose consumption and lactate production were measured using glucose assay kit and lactate assay kit, respectively. *P<0.05.

Figure 7

XIST positively regulated HK2 expression via sponging miR-653-5p. (A and B) Weston bolt assay was conducted to measure the protein abundance of HK2 in GI-LI-N and SK-N-BE(2) cells transfected with si-NC, si-XIST, si-XIST + anti-miR-NC, or si-XIST + anti-miR-653-5p. *P<0.05.